DOI: 10.1002/ejic.200900873

Synthesis and Solid State Structures of the Hydrogen-Bonded Hexamolybdoplatinate(IV) Tetramer $[(PtMo_6O_{24})_4H_{23}]^{9-}$ and the Hexamolybdoplatinate(IV) Trimers $[(PtMo_6O_{24})_3H_{16}]^{8-}$ and $[(PtMo_6O_{24})_3H_{14}]^{10-}$

Victor W. Day,*[a] James C. Goloboy,[b] and Walter G. Klemperer*[b]

Keywords: Polyoxometalates / Hydrogen bonds / Platinum / Molybdenum

The $[(PtMo_6O_{24})_3H_{16}]^{8-}$, $[(PtMo_6O_{24})_3H_{14}]^{10-}$, and $[(PtMo_6O_{24})_4H_{23}]^{9-}$ anions have been crystallized as tetra-*n*-butylammonium and tetra-*n*-butylammonium/triethylammonium salts and structurally characterized using single-crystal X-ray diffraction techniques. Together with the $[(PtMo_6O_{24})_2H_7]^{9-}$ and $[(PtMo_6O_{24})_2H_9]^{7-}$ anions described by Lee and Sasaki in 1994, these anions form a homologous series of hydrogen-bonded aggregates where stacks of protonated $[\alpha\text{-}PtMo_6O_{24}]^{8-}$ anions are stabilized by hydrogen-bonding interactions.

Introduction

Sasaki, Lee, and Joo have reported a family of unusual salts of the protonated $[\alpha\text{-}PtMo_6O_{24}]^{8-}$ hexamolybdoplatinate anion (see Figure 1), $K_7[(PtMo_6O_{24})_2H_9]\cdot 6H_2O$,[1,2] $K_7[(PtMo_6O_{24})_2H_9]\cdot 11H_2O$,[2,3] and $(NH_4)_9[(PtMo_6O_{24})_2H_7]\cdot 3H_2O$,[1] where pairs of hexamolybdoplatinate anions are connected by sets of seven hydrogen bonds. In the present study, we report the crystallization and solid-state structures of the hydrogen-bonded hexamolybdoplatinate trimers $[(PtMo_6O_{24})_3H_{16}]^{8-}$ and $[(PtMo_6O_{24})_3H_{14}]^{10-}$ and the tetramer $[(PtMo_6O_{24})_4H_{23}]^{9-}$. This family of dimers, trimers, and tetramers forms a homologous series that offers a unique insight into the ability of polyoxometalates to form hydrogen-bonded aggregates.

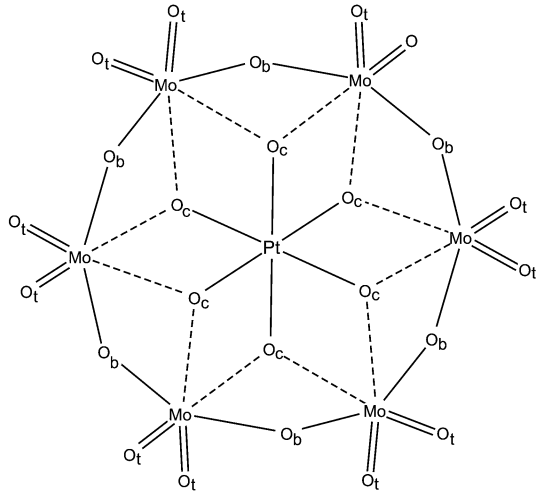

Figure 1. Line drawing of the $[\alpha\text{-}PtMo_6O_{24}]^{8-}$ anion. Terminal oxygen atoms are labeled O_t, doubly bridging oxygen atoms are labeled O_b, and triply bridging oxygen atoms are labeled O_c. The relatively short molybdenum–oxygen bonds to O_t oxygen atoms are represented by double lines, the relatively long molybdenum–oxygen bonds to O_b oxygen atoms are represented by dashed lines, and the remaining metal oxygen bonds are represented by single lines.

Results

Synthesis and Structure of the $[(PtMo_6O_{24})_4H_{23}]^{9-}$ Tetramer

The hexamolybdoplatinate tetramer was prepared by acidifying a solution of $K_2Pt(OH)_6$ plus six equivalents of K_2MoO_4 and adding tetra-*n*-butylammonium bromide to obtain a precipitate which was crystallized from acetonitrile/diethyl ether solution. This material, after removal from its mother liquor, washing, and drying, had the composition $[(PtMo_6O_{24})_4H_{23}][(n\text{-}C_4H_9)_4N]_9\cdot 4H_2O$ according to elemental analysis. Examination of material crystallized from acetonitrile/toluene solution using single-crystal X-ray diffraction techniques revealed an asymmetric unit containing two acetonitrile molecules, 4.5 tetra-*n*-butylammonium cations, half of a $[(PtMo_6O_{24})_4H_{23}]^{9-}$ anion, and a pair of oxygen atoms assigned to water molecules. The crystalline material was therefore formulated as $[(PtMo_6O_{24})_4H_{23}]$-

[a] Department of Chemistry, University of Kansas, 1251 Wescoe Hall Drive, Lawrence, KS 66045, USA
[b] Department of Chemistry, University of Illinois at Urbana-Champaign, 505 South Mathews Avenue, Urbana, IL 61801, USA
Supporting information for this article is available on the WWW under http://dx.doi.org/10.1002/ejic.200900873.

$[(C_4H_9)_4N]_9{\cdot}4H_2O{\cdot}4CH_3CN$ (**1**). A drawing of the rigorously centrosymmetric $[(PtMo_6O_{24})_4H_{23}]^{9-}$ anion and the two inversion-related pairs of water molecule oxygen atoms in compound **1** are shown in Figure 2; the atom labeling Scheme and metrical data for **1** are given in Figure S1 and Tables S1–S4 (see Supporting Information), respectively.

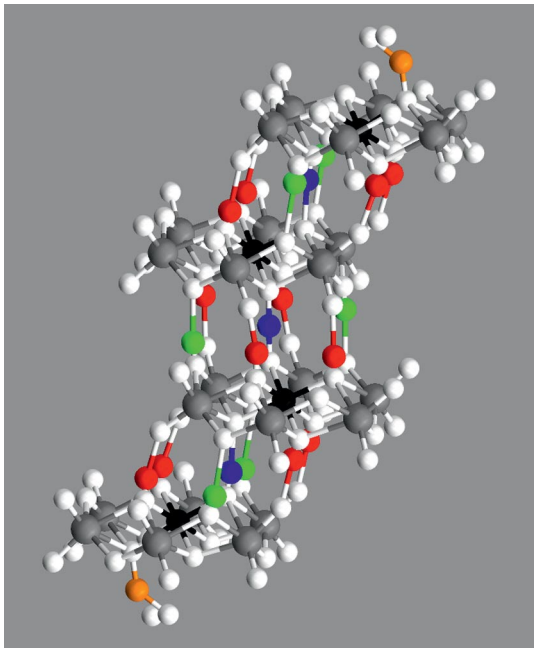

Figure 2. The C_i structure of the $[(PtMo_6O_{24})_4H_{21}(H_5O_2)_2]^{9-}$ anion in crystalline **1**. Molybdenum atoms are represented by grey spheres, platinum atoms by black spheres, and oxygen atoms by white spheres. Hydrogen atoms are represented by spheres color-coded according to the types of oxygen atoms they are bonded to: H33 atoms bonded to two triply bridging O_c oxygen atoms (see Figure 1 caption) are colored blue, H22 atoms bonded to two doubly bridging O_b oxygen atoms are colored green, H31 hydrogen atoms bonded to O_c and O_b oxygen atoms are colored red, and H3w hydrogen atoms bonded to O_c and Ow water oxygen atoms are colored orange.

All twelve crystallographically-independent hydrogen atoms in the rigorously centrosymmetric $[(PtMo_6O_{24})_4H_{23}]^{9-}$ tetramer in crystalline **1** were located with difference Fourier maps and included in the least-squares refinement as independent isotropic atoms whose parameters were allowed to vary. Pairs of adjacent $[PtMo_6O_{24}]^{8-}$ anions in this tetramer are linked by seven bridging hydrogen atoms that form a centered hexagon. The hydrogen atoms at the centers of these hexagonal arrays, colored blue in Figure 2, link two triply-bridging oxygen atoms labeled O_c in Figure 1 and are designated H33 hydrogen atoms. Two of the hydrogen atoms in each of the surrounding hexagons, those colored green in Figure 1, link two O_b doubly-bridging oxygen atoms and are designated H22 hydrogen atoms. The four remaining bridging hydrogen atoms, colored red in Figure 1, link O_c triply-bridging oxygen atoms and O_t terminal oxygen atoms and are designated H31 hydrogen atoms. The $[(PtMo_6O_{24})_4H_{23}]^{9-}$ tetramer also contains two terminally-bonded hydrogen atoms, those colored orange in Figure 1, that are bonded to O_c oxygen atoms and water molecule oxygen atoms, and these hydrogen atoms are designated H3w hydrogen atoms.

Both unsymmetrically and symmetrically bridging hydrogen atoms are observed in **1** (see Table S1). The H31 hydrogen atoms are all unsymmetrically bridging atoms, that is, they are strongly ("covalently") bonded to O_c triply-bridging oxygen atoms and weakly bonded ("hydrogen bonded") to O_t terminal oxygen atoms; the H22 hydrogen atoms are unsymmetrically bonded to O_b oxygen atoms in a similar fashion. The two peripheral H33 hydrogen atoms are also unsymmetrically bonded, but the central H33 atom lies on the anion's crystallographic inversion center and is symmetrically bonded to two O_c oxygen atoms with d(O–H) = 1.291(3) Å. Bonding to the H3w hydrogen atoms is also symmetric, with d(O–H) = 1.42(4) Å for both the O_c–H and Ow–H bonds. Because the O···O distance between the two adjacent water molecules (see Figure 2) is only 2.665(18) Å, they are presumably linked by bridging hydrogen atoms and together with the H3w hydrogen atom might form an $H_5O_2^+$ unit. Crystalline **1** might therefore be assigned the alternative formulation $[(PtMo_6O_{24})_4H_{21}][H_5O_2]_2[(C_4H_9)_4N]_9{\cdot}4CH_3CN$. If the relative strengths of the hydrogen bonds in the $[(PtMo_6O_{24})_4H_{21}(H_5O_2)_2]^{9-}$ unit can be estimated by comparing the O···O distances associated with each type of hydrogen atom (see Table S2), the hydrogen bonds involving H33, H31, and H3w hydrogen atoms, where d(O···O) = 2.543(4)–2.690(4) Å, appear to be stronger than the hydrogen bonds involving H22 hydrogen atoms, where d(O···O) = 2.755(4)–2.850(5) Å.

Comparison of metal–oxygen bond lengths in **1** shows the influence of protonation and hydrogen bonding on the geometry of $[PtMo_6O_{24}]^{8-}$ anions (see Table S3). Platinum–oxygen bond lengths are relatively constant with d(Pt–O) = 1.983(3) – 2.013(3) Å, but molybdenum–oxygen bond lengths show far greater variations. Consider first the effect of protonation and hydrogen bonding on Mo=O_t and Mo···O_c bond lengths in *trans* O_t=Mo···O_c units [see Figure 1 and Figure 3, (a)]. Lee and Sasaki[1] have pointed out that protonation of O_c oxygen atoms causes elongation of Mo···O_c bonds, and this trend is observed in the present structure as well: only those O_c oxygen atoms that are protonated have one or both Mo···O_c bond lengths greater than 2.3 Å. An equally pronounced elongation of O_t=Mo bonds upon formation of H···O_t=Mo hydrogen bonds is also evident in Figure 3, (a). Note also that formation of H···O_t=Mo hydrogen bonds not only elongates the M=O_t bond lengths but also compresses the *trans* Mo···O_c bond length in H···O_t=Mo···O_c, H···O_t=Mo···O_c···H, and H···O_t=Mo···O_c–H units. *Trans* bond length compression of the same type is observed for Mo–O_b bonds upon protonation by and hydrogen bonding to H22 hydrogen atoms as well. The effect of protonation and hydrogen bonding on bond lengths in $(–Mo–O_b–)_6$ rings is shown in Figure 4, (a) for peripheral $[PtMo_6O_{24}]^{8-}$ units and Figure 4, (b) for central $[PtMo_6O_{24}]^{8-}$ units. As noted previously by Lee and Sasaki,[1] protonation leads to elongation of Mo–O_b bonds,

and only those O_b oxygen atoms that are protonated have both Mo–O_b bond lengths longer than 2.0 Å. Protonation has a pronounced effect that induces a sequence of *trans* bond length alternations whereas hydrogen-bonding effects are minimal but nonetheless significant.

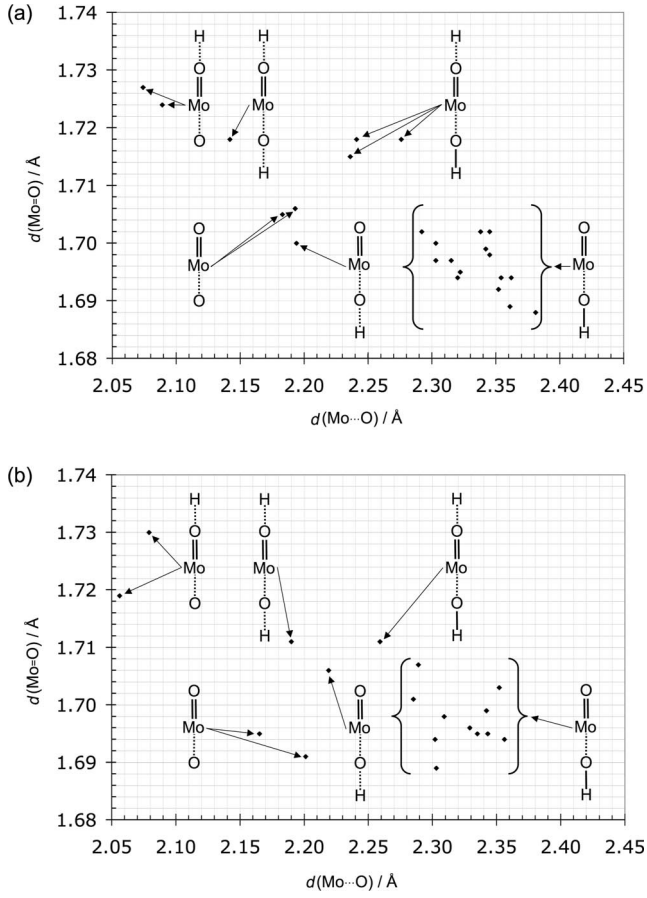

Figure 3. Graphs plotting the metal oxygen bond lengths for *trans*-O_t=Mo···O_c units in (a) crystalline **1** and (b) crystalline **2**. Estimated standard deviations for bond lengths in **1** and **2** are 0.003–0.004 and 0.006–0.009 Å, respectively.

Comparison of Mo–O–Mo bond angles in **1** also shows the influence of protonation and hydrogen bonding on the geometry of $[PtMo_6O_{24}]^{8-}$ anions (see Table S4), an effect noted previously by Lee and Sasaki[1] and Lee and Joo[3] for hexamolybdoplatinate dimers. For O_c oxygen atoms, Mo–O_c–Mo angles range from 88.5(1) to 93.3(1)° for protonated oxygen atoms and from 103.8(1) to 104.2(1)° for unprotonated oxygen atoms; for O_b oxygen atoms, Mo–O_b–Mo angles range from 108.2(2) to 110.9(1)° for protonated oxygen atoms and from 115.8(2) to 121.6(2)° for unprotonated oxygen atoms. In other words, protonation of oxygen atoms decreases their Mo–O–Mo bond angles by 4.9 to 15.7°, a very significant reduction considering that the estimated standard deviations for individual bond angles is 0.1–0.2°. Hydrogen bonding exerts a much smaller (and possible insignificant) influence on Mo–O–Mo angles for unprotonated O_b oxygen atoms: Mo–O_b–Mo angles range from 115.8(2) to 119.3(1)° for hydrogen bonded O_b···H–O_b oxygen atoms and from 119.9(1) to 121.6(2)° for unprotonated O_b oxygen atoms which are not O_b···H–O_b hydrogen bonded.

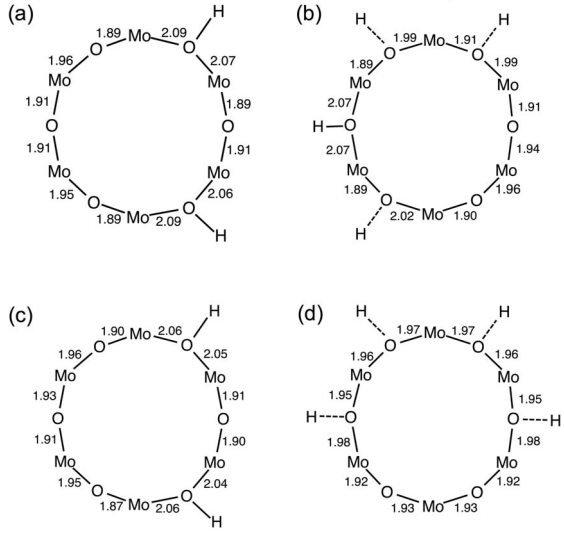

Figure 4. Diagrams showing the Mo–O_b bond lengths in $[PtMo_6O_{24}]^{8-}$ anions in crystalline **1** and **2**. Bond lengths for the peripheral and central anions in **1** are shown in (a) and (b), respectively. Bond lengths for the peripheral and central anions in **2** are shown in (c) and (d), respectively. Estimated standard deviations for all of the bond lengths are < 0.01 Å.

Note finally that the geometry of the platinum coordination polyhedra in **1** is significantly distorted from ideal octahedral geometry insofar as it is axially compressed by Mo···O_c bonding (see Figure 1): the O_c–Pt–O_c bond angles within the $Mo(O_c)_2Pt$ four-membered rings range from 82.1(1) to 83.9(1)°.

Synthesis and Structure of the $[(PtMo_6O_{24})_3H_{16}]^{8-}$ and $[(PtMo_6O_{24})_3H_{14}]^{10-}$ Trimers

Analytically pure bulk $[(PtMo_6O_{24})_3H_{15}][(C_4H_9)_4N]_6[(C_2H_5)_3NH]_3$ was prepared by reaction of $[(PtMo_6O_{24})_4H_{21}][(n\text{-}C_4H_9)_4N]_9\cdot 4H_2O$ with a large excess of triethylamine in acetonitrile solution. However, single crystals having this composition were not be obtained. Crystallization from acetonitrile/toluene solution yielded compound **2** which, according to a single-crystal X-ray structure determination (see below), was a solvated salt of the $[(PtMo_6O_{24})_3H_{16}]^{8-}$ anion, namely, $[(PtMo_6O_{24})_3H_{16}][(C_4H_9)_4N]_7[(C_2H_5)_3NH]\cdot 6CH_3CN\cdot 2H_2O$. Crystallization from acetonitrile/diethyl ether yielded a different compound denoted **3**, which contained the $[(PtMo_6O_{24})_3H_{14}]^{10-}$ anion according to the single-crystal X-ray diffraction study described below. The bulk sample therefore might not contain the $[(PtMo_6O_{24})_3H_{15}]^{9-}$ anion but might instead contain salts of the $[(PtMo_6O_{24})_3H_{16}]^{8-}$ and $[(PtMo_6O_{24})_3H_{14}]^{10-}$ anions in equal amounts.

All of the non-hydrogen atoms in **2** were located X-ray crystallographically, but because the quality of the diffraction data was considerably worse than the data for **1**, hydro-

gen atoms could not be located. Anion protonation sites could nonetheless be determined from protonation-induced metal–oxygen bond length elongations of the type noted above for compound **1**: O_c oxygen atoms having one or both Mo–O_c bond lengths ≥ 2.3 Å and O_b oxygen atoms having both Mo–O_b bond lengths ≥ 2.0 Å were assumed to be protonated. The rigorously C_2-symmetric structure shown in Figure 5 was generated using idealized hydrogen atom positions assuming idealized sp^2 hybridization at O_b oxygen atoms, idealized sp^3 hybridization at O_c oxygen atoms, and 0.84-Å O–H bond lengths. The atom labeling Scheme and metrical data for **2** are given in Figure S2 and Tables S5–S7, respectively.

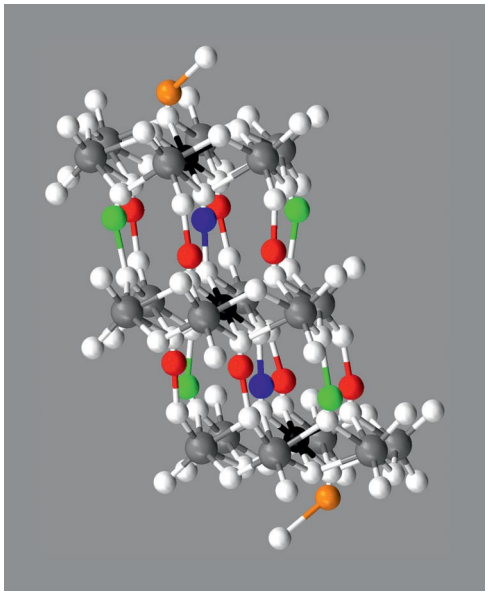

Figure 5. The C_2 structure of the $[(PtMo_6O_{24})_3H_{16}(H_2O)_2]^{9-}$ anion in crystalline **2**. Atoms are color-coded as described in the Figure 2 caption. Idealized hydrogen atom positions were generated as described in the text.

As shown in Figure 5, pairs of adjacent $PtMo_6O_{24}^{8-}$ anions in the hexamolybdoplatinate trimer are each linked by seven bridging hydrogen atoms of the same types observed in the tetramer, namely, one H33, two H22 and four H31 hydrogen atoms. Furthermore, the two peripheral $PtMo_6O_{24}^{8-}$ anions are each bonded to an H3w hydrogen atom, which is presumably hydrogen bonded to a water molecule [d(O···O) = 2.80(2) Å] as in the tetramer. The effects of protonation and hydrogen bonding on Mo=O_t and Mo–O_c bond lengths in **2** is shown in Figure 3, (b), where the same trends are observed as those noted above for the tetramer [see Figure 3, (a)]: protonation of O_c oxygen atoms lengthens Mo···O_c bonds; hydrogen bonding to O_t oxygen atoms lengthens Mo=O_t bonds and compresses Mo···O_c bonds in *trans* O=Mo···O units. The effects of protonation and hydrogen bonding on Mo–O_b bond lengths in the peripheral and central $PtMo_6O_{24}^{8-}$ units in **2** are shown in Figure 4, (c) and Figure 4, (d), respectively. Here, protonation induces sequences of bond length alternations of the type noted above for the tetramer; hydrogen-bonding effects, although relatively small, are nonetheless evident from small bond length elongations. As was the case for the hexamolybdoplatinate tetramer, Pt–O bond lengths are relatively constant with d(Pt–O) = 1.993(7)–2.028(7) Å, and O_c–Pt–O_c bond angles within the $Mo(O_c)_2Pt$ four-membered rings deviate significantly from their ideal values of 90° and range from 81.1(4) to 84.3(3)°. Also, the O···O distances associated with hydrogen bonds suggest that the hydrogen bonds involving H33 and H31 hydrogen atoms, where d(O···O) = 2.55(1)–2.58(1) Å, are stronger than the hydrogen bonds involving H22 hydrogen atoms, where d(O···O) = 2.71(1)–2.77(1) Å.

The X-ray diffraction data collected from crystalline **3** was of poor quality. It was possible to locate and refine all of the metal and oxygen atoms in a $PtMo_6O_{24}^{8-}$ trimer; five tetra-*n*-butylammonium cations, three triethylammonium cations, and ten solvent molecules could also be identified. However, none of the hydrogen atoms, several carbon atoms in the tetra-*n*-butylammonium cations, and numerous other atoms were not located: 21% (2210 Å^3)[4] of the unit cell was "empty." This space was presumably filled by disordered atoms of the remaining cations and/or solvent molecules. Because a total of 13 carbon atoms for the fourth and fifth tetra-*n*-butylammonium cations in the asymmetric unit of **3** could not be located from difference Fourier maps and

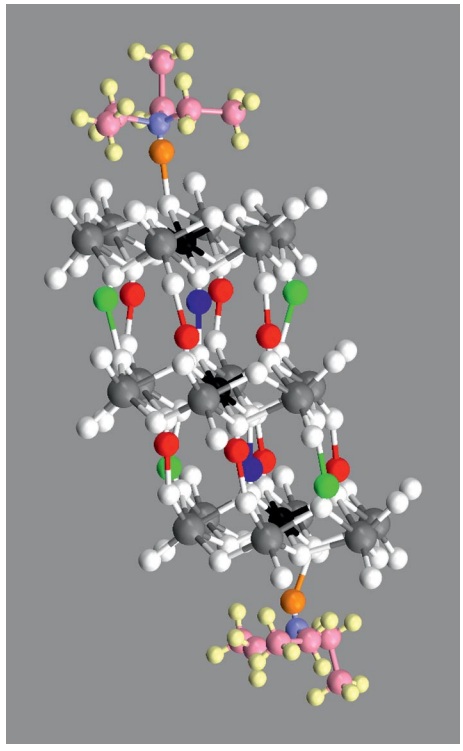

Figure 6. The C_1 structure of the $\{(PtMo_6O_{24})_3H_{14}[(C_2H_5)_3NH]_2\}^{8-}$ anion in crystalline **3**. In the triethylammonium cations, nitrogen atoms are represented by light blue spheres, hydrogen atoms bonded to carbon atoms by light yellow spheres, hydrogen atoms bonded to nitrogen atoms by orange spheres, and carbon atoms by light red spheres. The remaining atoms are color-coded as described in the Figure 2 caption. Idealized hydrogen atom positions were generated as described in the text.

each non-hydrogen atom in an organic crystal occupies an average volume of about 17 Å^3,[5] these missing atoms could account for about 442 Å^3 (2 asymmetric units/unit cell × 13 non-hydrogen atoms/asymmetric unit × 17 Å^3/non-hydrogen atom) of this "empty" space. The additional void volume could accommodate about 104 non-hydrogen atoms, more than enough to account for the two additional cations required to balance the charge of a $[(PtMo_6O_{24})_3H_{14}]^{10-}$ anion.

The structure of the $[(PtMo_6O_{24})_3H_{14}]^{10-}$ anion in **3** is shown in Figure 6, where protonation sites were assigned and idealized hydrogen atom positions were generated as described above for **2**. Metrical data for **3** are summarized in Tables S8–S10. Note that the positions occupied by terminally-bonded hydrogen atoms in **2** are occupied by hydrogen-bonded triethylammonium cations in **3**, where d(N···O) = 2.75(2) and 2.76(2) Å. The structure determination of **3** was insufficiently precise to allow for detailed analysis of structural effects of the type noted for **1** and **2** in Figures 3 and 4.

Discussion

The idealized line drawings of the $[(PtMo_6O_{24})_2H_9]^{7-}$ dimer,[3] the $[(PtMo_6O_{24})_3H_{16}]^{8-}$ trimer in **2** and the $[(PtMo_6O_{24})_4H_{23}]^{9-}$ tetramer in **1** shown in Figures 7, 8, and 9, respectively, show how the three hydrogen-bonded oligomers comprise a homologous series. In each case, nearest neighbor $[PtMo_6O_{24}]^{8-}$ anions are linked pairwise by seven bridging hydrogen atoms, of which four H31 hydrogen atoms link a triply bridging oxygen atom in one of the anions to a terminal oxygen atom in the other, two H22 hydrogen atoms link doubly-bridging oxygen atoms, and one H33 hydrogen atom links triply-bridging oxygen atoms. The $[(PtMo_6O_{24})_2H_7]^{9-}$ dimer[1] and the $[(PtMo_6O_{24})_3H_{14}]^{10-}$ trimer in **3** are also part of this series, possessing the full complement of bridging hydrogen atoms but lacking both terminal H3w hydrogen atoms. There is, however, an ambiguity in the dimer and tetramer structures insofar as both are crystallographically centrosymmetric such that the central H33 hydrogen atoms are apparently symmetrically bonded to two oxygen atoms. In each case the O_c–H33–O_c oxygen–oxygen distance atom is greater than 2.5 Å, a value at odds with the shorter distances normally associated with symmetric hydrogen bonds.[6–8] This suggests the presence of "apparently symmetric"[9] hydrogen bonds, that is, unsymmetric hydrogen bonding where crystallographic disorder or fluxional behavior yields a centrosymmetric structure when in fact, the hydrogen bond is unsymmetric,[10,11] the position adopted by Lee and Sasaki[1] and by Lee and Joo.[3] The same considerations apply to the H3w hydrogen atoms in $[(PtMo_6O_{24})_4H_{23}]^{9-}$, where d(O···O) = 2.599 Å, and this ambiguity implies an ambiguity in the formulation of compound **1** as either $[(PtMo_6O_{24})_4H_{23}][(C_4H_9)_4N]_9 \cdot 4H_2O \cdot 4CH_3CN$ or $[(PtMo_6O_{24})_4H_{21}][H_5O_2]_2[(C_4H_9)_4N]_9 \cdot 4CH_3CN$ (see above).

The metrical data available for the platinomolybdate trimer and tetramer provide detailed information regarding the effect of protonation and hydrogen bonding on the D_{3d}-symmetric $[PtMo_6O_{19}]^{8-}$ anion (see Figure 1). Data presented in Figure 3 raise an interesting possibility for hydrogen bonding in these species, namely, cooperative (and anticooperative) hydrogen bonding. Comparison of the data for (*trans*) O_t=Mo···O_c–H units and H···O_t=Mo···O_c–H units shows that hydrogen bonding to O_t oxygen atoms not only increases the O_t=Mo bond length but also decreases the Mo···O_c bond length, presumably weakening the O_c–H bond and creating a better hydrogen-bond donor, a potentially cooperative effect. A similar effect is observed for the

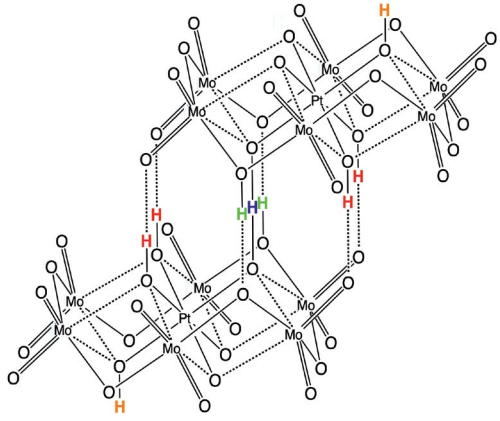

Figure 7. Line drawing of the $[(PtMo_6O_{24})_2H_9]^{7-}$ dimer. Metal–oxygen bonds are represented as described in the Figure 1 caption, short ("covalent") hydrogen–oxygen bonds are represented by single lines, and long hydrogen–oxygen bonds ("hydrogen bonds") are represented by dashed lines. Hydrogen atoms are color-coded as described in the Figure 2 caption.

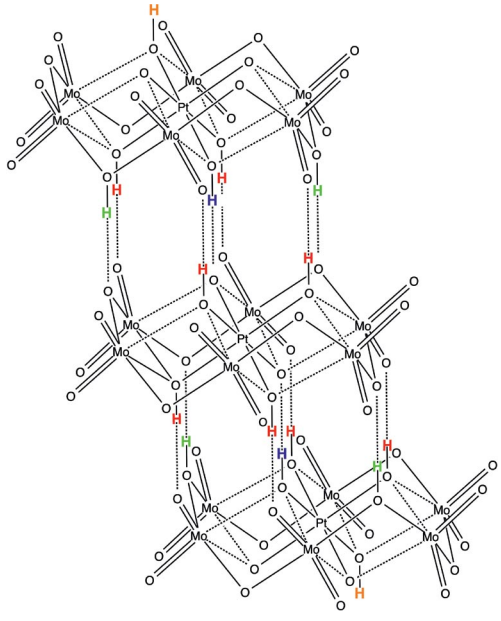

Figure 8. Line drawing of the $[(PtMo_6O_{24})_3H_{16}]^{8-}$ trimer. For explanation of the bonding scheme see the Figure 7 caption; for explanation of the hydrogen atom coloring scheme, see the Figure 2 caption.

O_t=Mo···O_c···H units, where hydrogen bonding to O_t renders the O_c oxygen atoms poorer hydrogen-bond acceptors, a potentially anticooperative effect. Because the X-ray crystallographically-determined hydrogen atom positions are unreliable, these effects are not observable in the present study but might be confirmed by spectroscopic measurements. Note also that the H3w oxygen atoms in the dimer, trimer, and tetramer structures in principal have three O_c oxygen atoms as potential protonation sites, but in each case protonation occurs at the unique O_c oxygen atom *trans* to only Mo=O_t (as opposed to Mo=O_t···H) groups, presumably because hydrogen bonding decreases the O_c atom basicity. Another type of *trans* effect is observed for *trans* O_b–Mo–O_b units, where sequences of *trans* bond length alternations are observed upon protonation of O_b oxygen atoms (see Figure 4). A similar trend was noted for the $[IMo_6O_{24}]^{5-}$ anion upon protonation of its O_b oxygen atoms.[12]

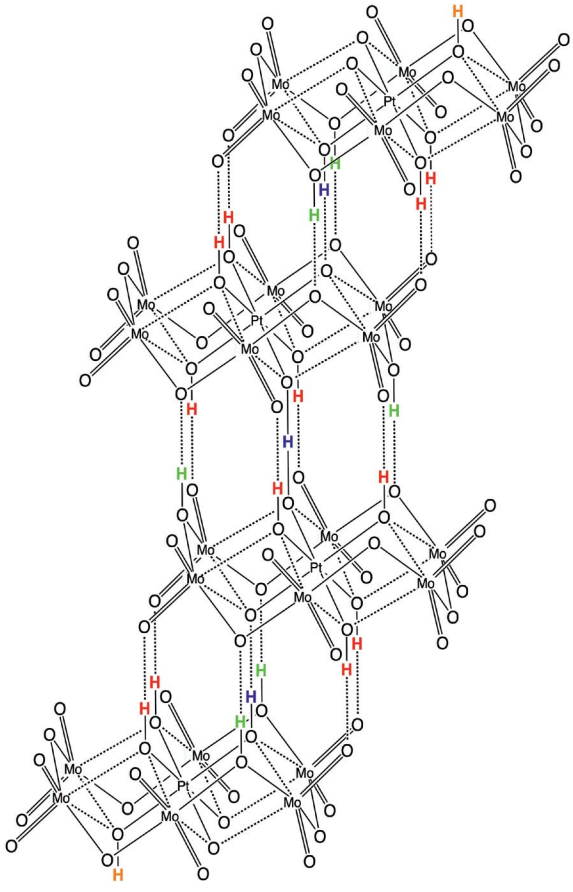

Figure 9. Line drawing of the $[(PtMo_6O_{24})_4H_{23}]^{9-}$ tetramer. For explanation of the bonding scheme see the Figure 7 caption; for explanation of the hydrogen atom coloring scheme, see the Figure 2 caption.

Formation of the homologous series of hydrogen-bonded oligomers shown in Figures 7, 8, and 9 is possible because two different types of oxygen atoms, the O_c and O_b oxygen atoms, have comparable basicities and can both serve as protonation sites. The relative basicities of the O_b and O_c atoms is largely determined by the oxidation state of the heteroatom in 1:6 heteropolymolybdates: the $[I^{VII}Mo_6O_{24}H]^{5-}$ and $[I^{VII}Mo_6O_{24}H_2]^{4-}$ anions are protonated at O_b oxygen atoms,[12] the $[M^{II}Mo_6O_{24}H_6]^{4-}$ and $[M^{III}Mo_6O_{24}H_6]^{3-}$ anions are protonated exclusively at O_c oxygen atoms,[13] and $[Pt^{IV}Mo_6O_{24}H_n]^{(8-n)-}$ anions are protonated at both O_b and O_c oxygen atoms.[1,3,14–18] Expansion of the present family of hydrogen-bonded platinomolybdate aggregates to include other 1:6 heteropolymolybdates and -tungstates[13] should therefore be possible through proper choice of the heteroatom oxidation state.

Experimental Section

Reagents, Solvents, and Analytical Procedures: Water was deionized using a Barnstead Nanopure II water purification system. Platinum(II) chloride, potassium molybdate, 85% potassium hydroxide pellets, calcium hydride, hydrochloric acid, nitric acid, ethanol, toluene, and diethyl ether were obtained from commercial sources and used as received without further purification. Acetonitrile was stirred over CaH_2 prior to use. Tetrabutylammonium bromide (Aldrich) was recrystallized from a saturated aqueous solution cooled to 0°. Triethylamine (Aldrich) was refluxed over CaH_2 and distilled from CaH_2 immediately prior to use. Infrared spectra were recorded on a Perkin–Elmer Series 1600 FT-IR spectrometer. Elemental analyses were performed at the University of Illinois Microanalytical Laboratory.

Preparation of H_2PtCl_6:[19] ***WARNING!*** Aqua regia is extremely corrosive and should be used in the *back* of a fume hood. An aqua regia solution was prepared by adding 75 mL of concd. HNO_3 to 225 mL of concd. aqueous HCl contained in a 500 mL round-bottomed flask. The flask was placed in an silicone oil bath, the flask was fitted with a water-cooled glass condenser, and the oil bath was heated to 75 °C. As the solution began to turn brown and bubble, 10 g $PtCl_2$ was added by stepwise with stirring over a period of 5 min. A clear solution was obtained by refluxing this mixture in a 115 °C oil bath for 2 d. The orange-brown solution was filtered through Whatman 42 filter paper, poured into a 400 mL beaker, and evaporated down to a volume of about 10 mL on a hot plate, making sure not to evaporate so much water that precipitates were formed (solid H_2PtCl_6 is susceptible to decomposition at elevated temperatures). Then 30 mL of concd. HCl were added, causing gas evolution, and the volume was once again reduced to about 10 mL by evaporation on the hot plate. This acidification/evaporation procedure was repeated until gas evolution was no longer observed upon acidification; two or three repetitions usually sufficed. The orange solution was then removed from the hot plate. An orange crystalline mass of H_2PtCl_6 formed upon cooling the solution to ambient temperature.

Preparation of $K_2Pt(OH)_6$:[20,21] A Teflon® beaker was filled with 350 mL of 6 M aqueous KOH, and the H_2PtCl_6 sample prepared above dissolved in 200 mL water was added, forming a yellow solution and a yellow precipitate. The mixture was heated on an oil bath with stirring at 95 °C for 18 h, and its volume was maintained by adding water periodically. The yellow-orange solution gradually became yellow-green as all the precipitate dissolved. The resulting solution was then cooled to room temperature. A 100 mL portion of the solution was poured into a polyethylene beaker and 150 mL of ethanol was added over the course of about 2 min with stirring. The yellow precipitate which formed was collected by vacuum filtration through a medium glass frit and washed with 30 mL water followed by 30 mL ethanol. The procedure was repeated (scaled for

the 50 mL portion) until all of the platinum solution had been used, and 14.7 g total of a light yellow powder was obtained. Crystalline $K_2Pt(OH)_6$ was obtained by dissolving 1 g of the crude product in 18 mL 4 M aqueous KOH in a Nalgene® beaker at room temperature and slowly evaporating the solution in a dessicator over KOH until yellow cubic crystals were obtained. In order to minimize cocrystallization of KOH, crystals were collected after about 6 mL of water had evaporated (after about 1 d). Crystals were collected by filtration, washed with 5 mL of ice-cold water, and dried under vacuum, yielding 800–900 mg of purified material. A total of 12.1 g of $K_2Pt(OH)_6$ (82% yield) was collected in this fashion.

Preparation of $[(PtMo_6O_{24})_4H_{23}][(n\text{-}C_4H_9)_4N]_9\cdot 4H_2O$: A solution of $K_2Pt(OH)_6$ (1.00 g , 2.66 mmol) in 133 mL water was prepared in a Nalgene® beaker. Another solution of K_2MoO_4 (3.807 g; 15.98 mmol) in 133 mL water was prepared in another Nalgene® beaker, and the two solutions were combined. The resulting yellow solution was stirred for 1 h and filtered by pouring through a plastic syringe packed with glass wool. The solution was then acidified to pH 2.32 by rapid addition of 30 mL 1 M (30 mmol) aqueous HNO_3, which caused the solution to turn a deep yellow then light yellow, followed by dropwise addition of 4.4 mL 1 M (4.4 mmol) aqueous HNO_3. This solution was stirred for three hours and again filtered by pouring through a plastic syringe packed with glass wool. Next, tetrabutylammonium bromide (2.14 g, 6.63 mmol) was added to the solution with stirring, immediately forming a precipitate, which was collected by vacuum filtration through a fine glass frit. After washing with 20 mL water and 20 mL diethyl ether, 2.51 g of a light tan solid was collected. The crude product was purified by dissolving in 5 mL acetonitrile, removing insoluble particles by filtration through a fine glass frit, and reprecipitating with 20 mL diethyl ether. A yellow solid (2.01 g) was collected after washing with diethyl ether and was dried in air on a vacuum filter. Crystals were obtained by dissolving 0.500 g of this material in 2 mL acetonitrile, adding 1 mL diethyl ether, and storing at 0 °C for 1–2 d until yellow needle-shaped crystals appeared. 1.09 g of crystalline product (24% yield based on Pt) was collected in total. The final product was very soluble in acetonitrile (0.1 M), slightly soluble in dichloromethane, and insoluble in chloroform. $C_{144}H_{355}Mo_{24}N_9O_{100}Pt_4$ (6896.27): calcd. C 25.08, H 5.19, N 1.83, Pt 11.32, Mo 33.39; found C 25.19, H 4.98, N 1.88, Pt 11.15, Mo 33.58. IR (KBr pellet, 1000–450 cm^{-1}): $\tilde{\nu}$ = 950 (s), 923 (s), 904 (s), 880 (s), 802 (w), 710 (s), 681 (m), 634 (s), 563 (m), 525 (m).

Preparation of $[(PtMo_6O_{24})_3H_{15}][(C_4H_9)_4N]_6[(C_2H_5)_3NH]_3$: A sample of $[(PtMo_6O_{24})_4H_{23}][(n\text{-}C_4H_9)_4N]_9\cdot 4H_2O$ (250 mg, 0.022 mmol) was dissolved in 1 mL acetonitrile. 5.10 μL triethylamine (0.022 mmol) was added to the solution with stirring every five minutes until 23 equiv. had been added. A slight yellow precipitate formed after 10 equiv. had been added. The solution was filtered through a fine glass frit, and 10 mL ether was added to the yellow filtrate, causing formation of a yellow precipitate which was collected by vacuum filtration through a fine glass frit. After drying under vacuum, 0.144 g of a light yellow solid was obtained. Yellow crystals were obtained by slow diffusion of diethyl ether into solutions containing 0.032 g of the crude product in 2 mL acetonitrile. Crystals obtained in this fashion were collected on a glass filter frit, air dried for 18 h, and combined to give a total of 0.087 g product in 47% yield based on Pt. $C_{114}H_{279}Mo_{18}N_9O_{72}Pt_3$ (5240.64): calcd. C 26.12, H 5.37, N 2.41; found C 25.87, H 5.14, N 2.37. IR (KBr pellet, 1000–450 cm^{-1}): $\tilde{\nu}$ = 942 (m), 918 (s), 902 (s), 876 (m, sh) 702 (s), 635 (s), 581 (m), 563 (m), 527 (m).

X-ray Crystallography: Crystalline **1** was obtained by following the initial steps of the preparation of $[(PtMo_6O_{24})_4H_{23}][(n\text{-}C_4H_9)_4N]_9\cdot 4H_2O$ given above but using 38 as opposed to 13 equiv. of nitric acid and crystallizing the crude precipitate from acetonitrile/toluene by dissolving 0.150 g in 5 mL acetonitrile, filtering the solution through a fine glass frit to remove a small amount of insoluble material, adding 5 mL of toluene, and capping the vial. Yellow, needle-shaped crystals were observed on the bottom of the vial after six days at ambient temperature. Crystalline **2** was obtained as described above in the preparation of $[(PtMo_6O_{24})_3H_{15}][(C_4H_9)_4N]_6[(C_2H_5)_3NH]_3$. Crystalline **3** was obtained by dissolving 0.045 g of crude product from the preparation of $[(PtMo_6O_{24})_3H_{15}][(C_4H_9)_4N]_6[(C_2H_5)_3NH]_3$ in 3 mL of acetonitrile, adding 5 mL of toluene, and shaking the solution to dissolve the small amount of precipitate that formed. Crystals were formed after three days.

Crystallographic information for all three structures is given in Table 1. Full hemispheres of diffracted intensities (1850 frames with an ω scan width of 0.30°) were measured for single-domain specimens of all three compounds using graphite-monochromated Mo-K_α radiation (λ = 0.71073 Å) on a Bruker SMART APEX CCD Single Crystal Diffraction System using Bruker SMART Version 5.054 software. Frame counting times and the number of peak centers used to determine final lattice constants and orientation matrices for each crystal are given in Table 1. X-rays for each study were provided by a fine-focus sealed X-ray tube operated at 50 kV and 30 mA or 35 mA. Integrated reflection intensities for all structures were produced using the Bruker SAINT Version 6.01 software. The data sets were corrected empirically for variable absorption effects using equivalent reflections.[22] The Bruker software package SHELXTL was used to solve each structure using "direct methods" techniques. All stages of weighted full-matrix least-squares refinement were conducted using F_o^2.

The final structural model for **1** incorporated anisotropic thermal parameters for all non-hydrogen atoms and isotropic thermal parameters for all hydrogen atoms of the anions, tetra-*n*-butylammonium (TBA) cations, and acetonitrile solvent molecules. Hydrogen atoms were not included for the water molecules. The twelve independent hydrogen atoms for the tetrameric anion in **1** were located from a difference Fourier map and included in the structural model as independent isotropic atoms whose parameters were allowed to vary in least-squares refinement cycles. All methyl groups for the cations and acetonitrile solvent molecules in **1** were incorporated into the structural model as rigid groups (using idealized sp^3-hybridized geometry and a C–H bond length of 0.98 Å) with a "staggered" orientation. The remaining hydrogen atoms in **1** were included into the structural model as idealized atoms (assuming sp^3-hybridization of the carbon atoms and a C–H bond length of 0.99 Å). The isotropic thermal parameters of all cation and solvent hydrogen atoms for **1** were fixed at values 1.2 (nonmethyl) or 1.5 (methyl) times the equivalent isotropic thermal parameter of the carbon atom to which they are covalently bonded.

The final structural models for **2** and **3** incorporated anisotropic thermal parameters whenever possible for non-hydrogen atoms of the anions. When anisotropic thermal parameters for an oxygen atom in the anions of **2** and **3** refined to physically unreasonable values, mild restraints were imposed or an isotropic thermal parameter was utilized in the refinement. Mild restraints were placed on the anisotropic thermal parameters for anion oxygen atoms O11a, O16a and O26a in **3**. Isotropic thermal parameters were used for the non-hydrogen atoms of the disordered triethylammonium (TEAH) cation and solvent atoms C5s, C6s and O1w in **2** and the following non-hydrogen atoms in **3**: C413, C414, C422, C423, and C424 for the fourth cation; N5, C511, C512, C513, C521, C531, and C532 for the fifth cation; all five non-hydrogen atoms for the

Table 1. Crystal, collection and refinement data for **1**–**3**.

	1	**2**	**3**
Empirical formula	$C_{76}H_{183.50}Mo_{12}N_{6.5}O_{50}Pt_2$	$C_{130}H_{306}Mo_{18}N_{14}O_{74}Pt_3$	$C_{112}H_{275}Mo_{18}N_{13}O_{76}$ Pt_3
Formula weight	3530.25	5562.08	5332.64
Crystal system	monoclinic	monoclinic	triclinic
Space group	$C2/c$-C_{2h}^6 (No.15)	$C2/c$-C_{2h}^6 (No.15)	$P\bar{1}$-C_i^1 (No. 2)
a [Å]	36.760(3)	21.918(3)	18.821(2)
b [Å]	18.187(1)	31.919(5)	20.372(2)
c [Å]	38.027(2)	30.265(5)	30.381(3)
α [°]	90.000	90.000	89.625(2)
β [°]	92.049(2)	90.347(2)	85.167(2)
γ [°]	90.000	90.000	64.272(2)
V [Å^3]	25407(3)	21173(5)	10451(2)
Z	8	4	2
$d_{calcd.}$ [g cm^{-3}]	1.846	1.745	1.695
λ (Å)	0.71073	0.71073	0.71073
T [K]	193(2)	193(2)	193(2)
F(000)	13960	11064	5272
Absorption coefficient [mm^{-1}]	3.41	3.08	3.11
Absorption correction	Multi-scan	Multi-scan	Multi-scan
Max., min. transmission	1.000, 0.792	1.000, 0.629	1.000, 0.380
Frame time [s]	10	60	30
Peak centers for lattice constants	7996	8315	8558
θ range [°]	5.34–29.38	3.76–24.15	3.87–24.00
Reflections collected	105749	71163	48961
Independent reflections/R_{int}	32505/0.044	16864/0.090	30615/0.083
% Completeness	92.8	99.5	93.3
Data/restraints/parameters	32505/0/1350	16864/26/1042	30615/35/1783
R_1(obsd); wR_2(all)[a]	0.039; 0.092	0.074; 0.223	0.097; 0.290
GOF (F^2)	0.948	1.001	1.092

[a] $R_1 = \Sigma \, ||F_o| - |F_c|| / \Sigma \, |F_o|$; $wR_2 = \{\Sigma \, w(F_o^2 - F_c^2)^2 / \Sigma \, w(F_o^2)^2 \}^{1/2}$.

diethyl ether molecule; and the oxygen atoms for all three water molecules. The following non-hydrogen atoms in **3** could not be located from difference Fourier maps: five carbon atoms for the fourth TBA cation and eight carbons for the fifth TBA cation.

A free variable representing the length of a C–C single bond was included in the refinements for **2** and **3** to restrain selected segments of the TBA and TEAH cations. The TEAH cation in **2** is disordered about the crystallographic C_2 axis at –1/2, y, 1/4 in the unit cell; nitrogen atom N5 lies on the C_2 axis. The ethyl arms of this TEAH cation are therefore disordered. The values of 8 C–C and 4 N–C bond lengths and 14 tetrahedral angles in this TEAH cation and one TBA cation of **2** were restrained by requiring pairs of non-hydrogen atoms to have separations near idealized multiples of this free variable. This free variable refined to a final value of 1.498(2) Å for **2**. The values of 7 C–C and 4 N–C bond lengths and 6 tetrahedral angles in two TBA cations of **3** were similarly restrained to appropriate multiples of this free variable. This free variable refined to a final value of 1.600(5) Å for **3**.

Hydrogen atoms were incorporated at idealized sp^2- or sp^3-hybridized positions with an O–H bond length of 0.84 Å for the trimeric anions in **2** and **3**. All methyl groups for the TBA and TEAH cations as well as the CH_3CN and diethyl ether solvent molecules in **2** and **3** were incorporated into the structural model as rigid groups (using idealized sp^3-hybridized geometry and a C–H bond length of 0.98 Å) with a "staggered" orientation. The remaining cation and solvent (except water) hydrogen atoms were included into the structural model as idealized atoms (assuming sp^3-hybridization of the carbon and nitrogen atoms and N–H and C–H bond lengths of 0.93 and 0.99 Å, repectively). The isotropic thermal parameters of all hydrogen atoms for **2** and **3** were fixed at values 1.2 (nonmethyl) or 1.5 (methyl) times the equivalent isotropic thermal parameter of the carbon, nitrogen or oxygen atom to which they are covalently bonded.

CCDC-74628 (for **1**), -74629 (for **2**), and -74630 (for **3**) contain the supplementary crystallographic data for this paper. These data can be obtained free of charge from The Cambridge Crystallographic Data Centre via www.ccdc.cam.ac.uk/data_request/cif.

Supporting Information (see also the footnote on the first page of this article): Figure S1–S3, Tables S1–S10.

Acknowledgments

The synthetic work was supported by the U. S. Department of Energy, Division of Materials Sciences, under Award No. DEFG02-91ER45439, through the Frederick Seitz Materials Research Laboratory at the University of Illinois at Urbana-Champaign. The X-ray diffraction data was collected by Dr. Cynthia Day at Wake Forest University.

[1] U. Lee, Y. Sasaki, *Bull. Korean Chem. Soc.* **1994**, *15*, 37–45.
[2] The $K_{3.5}[H_{4.5}PtMo_6O_{24}]\cdot 3H_2O$ structure (**a**) described in ref.[1] and the $K_{3.5}[H_{4.5}PtMo_6O_{24}]\cdot 5.5H_2O$ structure (**b**) described in ref.[3] appear to be virtually the same structure. Transformation of the nonstandard triclinic cell for **a** to a standard triclinic cell gives the lattice constants 10.089Å × 12.001Å × 12.426Å × 69.25° × 69.27° × 83.44°; these closely resemble those reported for **b**. The transformed triclinic cell and the original triclinic cell for **a** have a volume of 1315.7Å^3, not 1332.2 Å^3 as reported in ref.[3]. Metal–oxygen bond lengths in **a** match those in **b** within two estimated standard deviations.
[3] U. Lee, H.-C. Joo, *Acta Crystallogr., Sect. E* **2007**, *63*, i11–i13.

[4] A. L. Spek, *PLATON: Program for the Geometrical Interpretation of Structural Data*, University of Utrecht, **1999**.
[5] P. Román, C. Guzmán-Miralles, A. Luque, *Acta Crystallogr., Sect. B* **1993**, *49*, 383–386.
[6] T. Steiner, W. Saenger, *Acta Crystallogr., Sect. B* **1994**, *50*, 348–357.
[7] Y. H. Mariam, R. N. Musin, *J. Phys. Chem. A* **2008**, *112*, 134–145.
[8] G. V. Yukhnevich, *Crystallogr. Rep.* **2009**, 184–189.
[9] G. C. Pimentel, A. L. McClellan, *Annu. Rev. Phys. Chem.* **1971**, *22*, 347–385 .
[10] W. C. Hamilton, *Annu. Rev. Phys. Chem.* **1962**, *13*, 19–40.
[11] J. A. Ibers, *Annu. Rev. Phys. Chem.* **1965**, *16*, 375–396.
[12] D. Honda, S. Ikegami, T. Inoue, T. Ozeki, A. Yagasaki, *Inorg. Chem.* **2007**, *46*, 1464–1470.
[13] M. T. Pope, *Heteropoly and Isopoly Oxometalates*, Springer-Verlag, Berlin, **1983**, p. 22.
[14] U. Lee, *Acta Crystallogr., Sect. C* **1994**, *50*, 1657–1659.
[15] U. Lee, H. C. Joo, *Acta Crystallogr., Sect. C* **2000**, *56*, e311–e312.
[16] U. Lee, H.-C. Joo, *Acta Crystallogr., Sect. E* **2004**, *60*, i61–i63.
[17] U. Lee, H.-C. Joo, *Acta Crystallogr., Sect. E* **2006**, *62*, i231–i233.
[18] U. Lee, H. C. Joo, *Acta Crystallogr., Sect. E* **2006**, *62*, i241–i243.
[19] L. Wohler, *Z. Elektrochem.* **1909**, *15*, 769–773.
[20] A. R. Powell, E. C. Davies, A. W. Scott, *Preparation and operation of platinum plating baths*; U. S. Pat. No. 1,906,178, April 25, **1933**.
[21] A. R. Powell, E. C. Davies, A. W. Scott, *Alkali metal platinates and their manufacture*, U. S. Pat. No. 1,906,179, April 25, **1933**.
[22] G. M. Sheldrick, *SADABS, Program for Empirical Absorption Correction of Area Detector Data*, University of Göttingen, **2002**.

Received: September 3, 2009
Published Online: November 11, 2009

